

The behavior of cesium adsorption on zirconyl pyrophosphate

Feng-Li Song¹ · Xiao-Wei Yang¹ · Xiao-Long Li¹ ·
Wei He¹ · Dan Lü¹ · Ji Que¹ · Chun-Long Zhang¹ ·
Shan-Gui Zhao¹ · Shi-Jun Wang¹ · Yun-Tao Liu¹

Received: 13 July 2015 / Revised: 9 September 2015 / Accepted: 17 September 2015 / Published online: 10 May 2016
© Shanghai Institute of Applied Physics, Chinese Academy of Sciences, Chinese Nuclear Society, Science Press China and Springer
Science+Business Media Singapore 2016

Abstract Zirconyl pyrophosphate (ZrP_2O_7) was prepared and Cs adsorption behavior was studied. Results show that the distribution coefficient of Cs adsorption on ZrP_2O_7 was about 2800 mL/g. Ion exchange capacity of ZrP_2O_7 was 0.35 mmol/g. In dynamic tests, Cs can be separated from other fission products very well by ZrP_2O_7 . The ZrP_2O_7 was stable both at high temperatures and in high concentration of nitric acid. The Cs adsorption by ZrP_2O_7 is a monolayer and chemical adsorption.

Keywords Zirconyl pyrophosphate · Adsorbent · Cesium

1 Introduction

A large number of high-level radioactive liquid wastes (HLLWs) are produced in spent nuclear fuel reprocessing. With complex composition and strong radioactivity, the final disposal of HLLWs has been of a great concern [1]. At present, the treatment method is vitrification of HLLWs. Partition–transmutation [2–5] can reduce the risk of long-term disposal of HLLWs. Chemical separation, a key technology of partition–transmutation, can not only combine with transmutation to reduce the harm of HLLWs, but also reduce the volume of waste to be disposed. ^{137}Cs , as a fission product that can strongly release the decay heat, needs to be separated from the HLLWs [6]. Also, ^{137}Cs can

be used as a radiation source in gamma ray well logging devices, flow meters, thickness gauges, etc.

The methods of cesium separation from HLLWs include co-precipitation [7], solvent extraction [8–12], ion exchange [13, 14], etc. While co-precipitation is of poor selectivity and solvent extraction is of poor radiation stability, inorganic ion exchange [15, 16], being advantageous in selectivity, radiation stability and thermal stability, is a desirable way to separate cesium. Multivalent metal phosphate especially zirconyl phosphate [17, 18] has received much attention for its good adsorption property to cesium. Zirconyl phosphate is of low adsorption capacity, but this can be increased by replacing phosphate with pyrophosphate. Many studies show that zirconyl molybdopyrophosphate (ZMPP) [19–23] ionic sieve can separate cesium from HLLWs in good selectivity and large ion exchange capacity. However, zirconyl pyrophosphate is more simple, and more suitable for large-scale industrial production in the future. In this paper, we report the synthesis of zirconyl pyrophosphate and its adsorption property study.

2 Experimental

2.1 Preparation of adsorbent [23]

Potassium pyrophosphate and $ZrOCl_2$ were mixed in acid solutions. After complete precipitation, the solution acidity was adjusted. After 24 h, the precipitate was filtrated. It was washed with water and dried at 40 °C. The product was treated with 1 mol/L HNO_3 (~20 mL of 1 mol/L HNO_3 for 1 g adsorbent). It was washed with water again and dried for use.

This work is supported by the Defense Advanced Research Project.

✉ Ji Que
quejiqueji@163.com

¹ Nuclear and Radiation Safety Center, Ministry of Environmental Protection, Beijing 100082, China

2.2 Adsorption and elution experiment

2.2.1 Determination of distribution coefficient and ion exchange capacity

Certain amount of the adsorbents was placed into a test tube, and ^{137}Cs solution was added (In determining the ion exchange capacity, ^{133}Cs solution using ^{137}Cs as tracer was added. The ^{133}Cs concentration was measured by the atomic emission spectrometry before adsorption). After the adsorption reached equilibrium, the activity was analyzed with gamma spectrometry before and after adsorption. The distribution coefficient (K_d , in mL/g) and ion exchange capacity (Q , in mmol/g) were calculated by Eqs. (1) and (2):

$$K_d = (C_0 - C)V/(Cm) = (A_0 - A)V/(Am), \quad (1)$$

$$Q = (C_0 - C)V/m = (C_0V/m)(1 - A/A_0), \quad (2)$$

where A_0 and A are counting rates of Cs in the aqueous phase before and after adsorption equilibration (cps), respectively; C_0 and C are Cs concentration in aqueous phase before and after adsorption equilibration, respectively (mol/L); V is volume of the aqueous phase (mL); and m is the weight of adsorbent (g).

2.2.2 Elution of cesium

A certain amount of adsorbents was placed into a test tube, and ^{137}Cs solution was added. After equilibrium, the activity was analyzed with single-channel gamma spectrometry before and after adsorption. The Cs concentration was represented as activity. The ZrP_2O_7 was washed, and the cesium was eluted by the higher concentration of acid (5, 6, 8 and 10 mol/L HNO_3). The activity after elution was analyzed with gamma spectrometry. The percentage elution was calculated by Eq. (3):

$$\text{Percentage elution} = C_2/(C_0 - C_1) = A_2/(A_0 - A_1), \quad (3)$$

where A_0 and A_1 are the counting rates of Cs in the aqueous phase before and after adsorption equilibration (cps). A_2 is the counting rates of Cs after elution (cps). C_0 and C_1 are the cesium concentration in the aqueous phase before and after adsorption equilibrium, respectively (mol/L). C_2 is the cesium concentration after elution (mol/L).

3 Results and discussion

3.1 Cs adsorption on ZrP_2O_7

3.1.1 Static experiments

Figure 1 shows the Cs distribution coefficient as function of adsorption equilibrium time. The Cs adsorption on

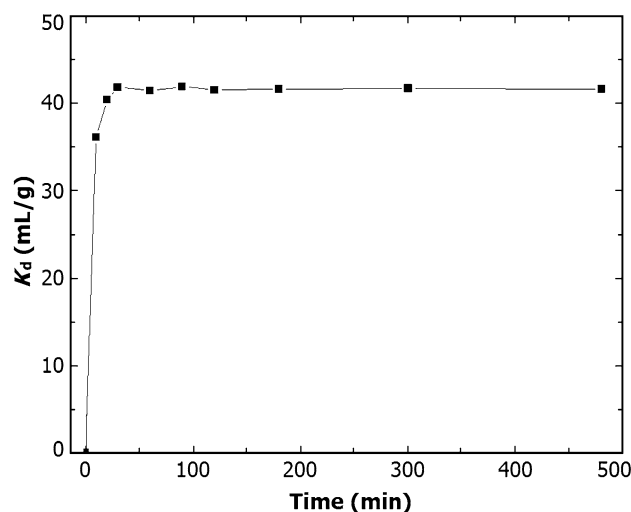


Fig. 1 Distribution coefficient of cesium (K_d) as function of adsorption equilibration time

Table 1 Percentages adsorption (A) and K_d in different concentrations of HNO_3

C_{HNO_3} (mol/L)	0.1	0.3	0.5	1.0	1.5	2.0	2.5
K_d ($\times 100$ mL/g)	28	10	6.7	4.7	3.4	2.8	2.2
%A	97	93	89	85	81	78	73

ZrP_2O_7 reaches equilibrium within 30 min. The adsorption rate is rapid.

The adsorption percentage and distribution coefficients at different HNO_3 concentrations are listed in Table 1. Both the adsorption percentage and distribution coefficient decrease with increasing HNO_3 concentrations.

At 2 mol/L HNO_3 , the adsorption percentage and distribution coefficient at $21^\circ\text{--}80^\circ$ are listed in Table 2. The adsorption distribution coefficients and adsorption rates decrease with increasing temperature.

For cesium adsorption at 2 mol/L HNO_3 , the cesium was eluted at 12°C , and the elution fractions were 46.7 and 62.4 % by 5 and 10 mol/L HNO_3 , respectively. And the elution fraction increased with elution temperature.

Portions of ZrP_2O_7 were weighed accurately and transferred into the test tubes, and then 5 and 10 mol/L HNO_3 , 0.5 and 1 mol/L NaOH , and 0.5 mol/L Na_2CO_3 solution were added, respectively. The test tubes were heated in a water bath and kept at 90°C for 2 h. The percentages of Cs adsorption cesium by ZrP_2O_7 before and after the treatment are listed in Table 3.

The results show that ZrP_2O_7 soaked with NaOH can hardly adsorb cesium, the percentage of Cs adsorption by ZrP_2O_7 soaked with HNO_3 decreases slightly, and ZrP_2O_7 is dissolved in 0.5 mol/L Na_2CO_3 . It can be seen that ZrP_2O_7 is stable at high temperature and in high HNO_3 concentration.

Table 2 Percentages adsorption (%A) and K_d at different temperatures

Temperature (°C)	21.1	39.1	59.1	70.0	80.0
K_d (mL/g)	244	127	54.7	38.0	22.4
%A	75.3	61.3	40.6	32.2	21.9

It is preliminary speculated that -OH are presented on surface of ZrP_2O_7 . Hydrogen of -OH may exchange with cesium ions so that ZrP_2O_7 can adsorb cesium. When ZrP_2O_7 is soaked with NaOH, the sodium ion exchanges with hydrogen of -OH, and cesium cannot be absorbed. This may be because zirconium of ZrP_2O_7 and carbonate can form a complex, so that it is dissolved in Na_2CO_3 .

3.1.2 Dynamic experiments

In static experiments, ZrP_2O_7 shows good adsorption property, but ^{137}Cs cannot be eluted well at room temperature. Furthermore, the metal ion is usually difficult to be eluted. Therefore, the Cs elution on ZrP_2O_7 is investigated in dynamic experiments.

3.1.2.1 Effect of nitric acid concentration on elution ZrP_2O_7 was packed into a column of 0.35 cm × 14 cm in slurry state. Then, ^{137}Cs solution flew through the column at a flow rate of 0.1 mL/min. Finally, cesium was eluted at 12 °C by 10 and 8 mol/L HNO_3 . The results are shown in Fig. 2. It can be seen that cesium is better eluted by 10 mol/L HNO_3 . This agrees with the static investigation. The Cs adsorption increases with decreasing HNO_3 concentration, and the elution increases with HNO_3 concentration.

3.1.2.2 Effect of temperature on elution ZrP_2O_7 was packed into a column of $\Phi 0.32$ cm × 11.5 cm in slurry state, and the ^{137}Cs solution in 2 mol/L HNO_3 flew through the column at a flow rate of 0.12 mL/min. Finally, cesium was eluted by 8 mol/L HNO_3 at 60 and 12 °C. The results are shown in Fig. 3. Cesium is better eluted at 60 °C. These agree with the static investigation. The Cs adsorption increases with decreasing temperature, and the elution increases with temperature.

3.1.2.3 Elution by 8 mol/L HNO_3 Although cesium elution by 10 mol/L HNO_3 is more efficient (Fig. 2), the acid

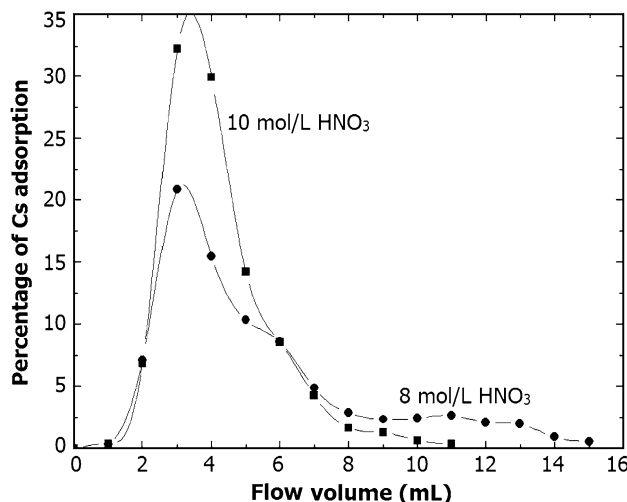


Fig. 2 Cs elution curves by HNO_3 of different concentrations at 12 °C

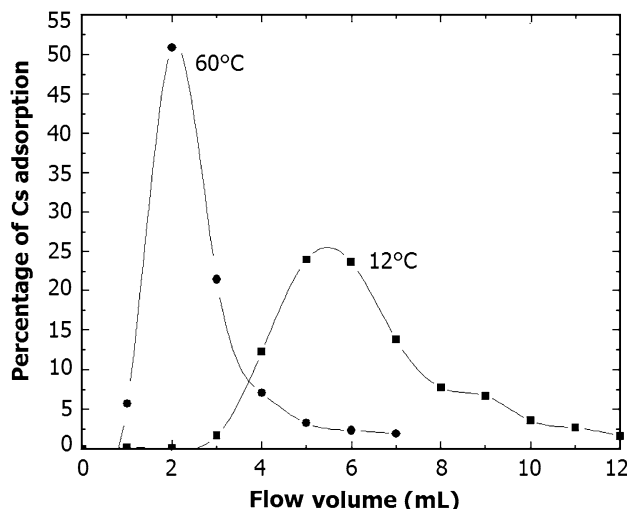


Fig. 3 Cs elution curves at different temperatures in 2 mol/L HNO_3

concentration is too high to protect equipment from corrosion. Therefore, we tried to decrease the acid concentration. ZrP_2O_7 was packed into a column of $\Phi 0.3$ cm × 11 cm in slurry state. The ^{137}Cs solution in 2 mol/L HNO_3 flew through the column at a rate of 0.1 mL/min. Finally, cesium was eluted by 8 mol/L HNO_3 at 60 °C. As shown in Fig. 4, cesium can be eluted completely.

Table 3 Percentage adsorption of cesium by ZrP_2O_7 before and after soaked with HNO_3 and NaOH

ZrP_2O_7	Before treated	5 mol/L HNO_3	10 mol/L HNO_3	0.5 mol/L NaOH	1 mol/L NaOH	0.5 mol/L Na_2CO_3
%A	85	78	83	3	4	Dissolved

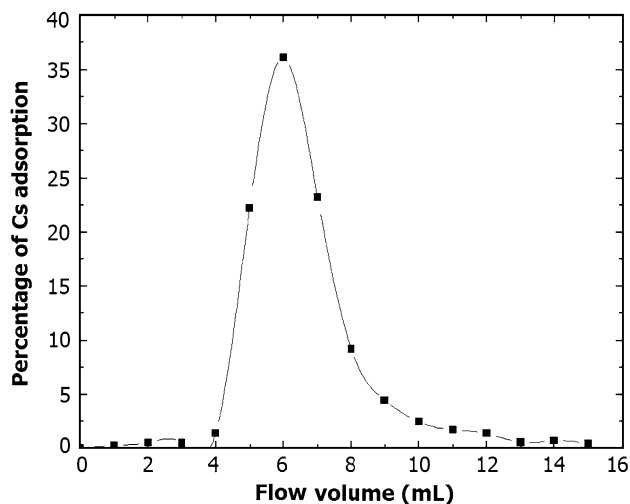


Fig. 4 Elution curve of cesium by 8 mol/L HNO₃ at 60 °C

3.1.2.4 Extracting Cs from dissolved solution of the irradiated uranium ZrP₂O₇ was packed into a column of $\Phi 0.3$ cm \times 11 cm in slurry state. The solution dissolved with irradiated uranium in 2 mol/L HNO₃ flew through the column at a rate of 0.4 mL/min. Then, the column was washed by 2 mol/L HNO₃. Finally, cesium was eluted by 8 mol/L HNO₃ at 60 °C. Activities of the U-dissolved solution, washed solution and eluted solution were measured by HPGE gamma spectrometry. The results are given in Table 4. Almost all the ¹³⁷Cs in the U-dissolved solution, and most of the ⁹⁵Zr and ⁹⁵Nb, were adsorbed by the column, but ¹⁴⁴Ce and ¹⁰⁶Ru were not. After being eluted, almost all ¹³⁷Cs was recovered in the solution, but ⁹⁵Zr and ⁹⁵Nb retained on the column. Cs can be separated from other fission products very well by ZrP₂O₇.

3.2 Adsorption mechanism

3.2.1 Adsorption isotherm

This kind of adsorption isotherm is often described by Langmuir adsorption theory. The isothermal equation of Langmuir adsorption theory is expressed as follows [24]:

$$Q = Q_m b C / (1 + b C) \quad (4)$$

where Q is the adsorption capacity (mmol/g), C is the measured metal concentration in aqueous phase (mmol/L), Q_m is the saturated metal concentration in aqueous phase (mmol/L) and b is a constant.

Equation (4) can be transformed to a linear equation as:

$$1/Q = 1/Q_m + 1/(bQ_m C) \quad (5)$$

If the Cs adsorption by ZrP₂O₇ can be described by Langmuir adsorption theory, the $1/Q$ should be linear with $1/C$. The relationship between $1/Q$ and $1/C$ of Cs adsorption on ZrP₂O₇ at 30 °C is shown in Fig. 5. The data are in a good linear correlation. This shows that the Cs adsorption on ZrP₂O₇ can be described by the Langmuir adsorption theory. Therefore, it is a monolayer adsorption. It may be chemical adsorption or physical adsorption. They should be identified by adsorption heat.

3.2.2 Adsorption heat

The plot of $\ln K_d$ as a function of $1/T$ is shown in Fig. 6, from which the adsorption heat can be estimated at -34.40 kJ/mol. The negative value shows the adsorption is an exothermic process, with which the adsorption distribution ratio decreases with increasing temperatures. And the value was in the range of chemical adsorption heat. So we concluded that the Cs adsorption on ZrP₂O₇ is chemical adsorption.

3.2.3 Experimental evidence of ion exchange reaction

The ion exchange of ZrP₂O₇ was investigated in low acid concentrations, so that the changes in pH in the aqueous phase before and after adsorption could be measured. The changes in hydrogen and cesium ion concentrations were compared before and after adsorption (Table 5). After adsorption, the cesium ion concentration decreased and the hydrogen ion concentration increased. Although the increase in hydrogen ion concentration (ΔC_H) is a little smaller than the decrease of the cesium ion concentration (ΔC_{Cs}), due to probably measurement

Table 4 Experimental data of extracting Cs from U-dissolved solution

Isotopes	Energy (keV)	Counts per second			Decontamination coefficient
		Irradiated uranium	Washed solution	Eluted solution	
⁹⁵ Zr	756.7	3.01	0.064	0.008	379
⁹⁵ Nb	765.8	9.06	0.256	0.110	82.9
¹⁴⁴ Ce– ¹⁴⁴ Pr	133.5	995	1062	0.270	3.71×10^3
	¹⁰⁶ Ru– ¹⁰⁶ Rh	511.82	55.8	57.0	
1.48×10^3					
¹³⁷ Cs	661.7	321	0.120	323	1

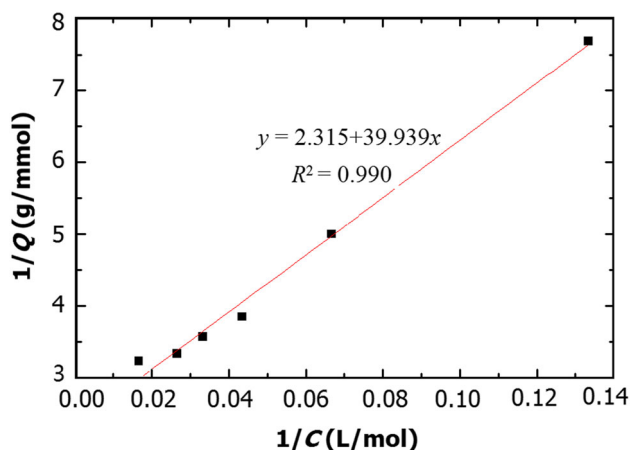


Fig. 5 Relationship between $1/Q$ and $1/C$ of Cs adsorption on ZrP_2O_7 at 30 °C

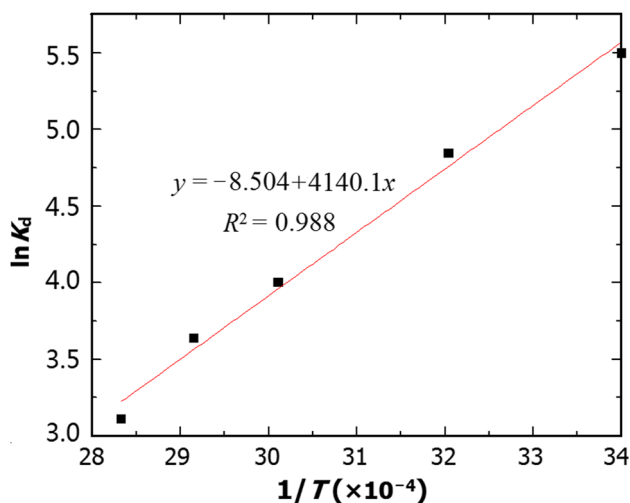


Fig. 6 Heat of Cs adsorption on ZrP_2O_7

Table 5 Cs and H ion concentrations (in mmol/L) in the solution before (B.) and after (A.) adsorption

C_{Cs}		C_H		ΔC_{Cs}	ΔC_H
B.	A.	B.	A.		
70.7	45.8	1.32	20.0	25.0	18.7

error, this suggests that hydrogen ions in the surface of ZrP_2O_7 are replaced by the cesium in the aqueous phase. So the adsorption is a chemical adsorption.

The reaction of $-OH$ presented on the surface of ZrP_2O_7 and Cs can produce hydrogen ions. So the concentration of nitric acid is high, and reverse reaction will be carried out. That explains why distribution coefficients decrease with increasing HNO_3 concentrations.

4 Conclusion

Zirconyl pyrophosphate (ZrP_2O_7) was synthesized by a simple co-precipitation method. It has a good chemical stability both at high temperature and in high concentration of nitric acid. The static experiments show that the Cs adsorption distribution coefficient is 2800 mL/g and the ion exchange capacity is 0.35 mmol/g. In dynamic tests, Cs can be well separated from other fission products. The Cs adsorption by ZrP_2O_7 is a monolayer and chemical adsorption. The adsorption mechanism is that the hydrogen in the surface of ZrP_2O_7 is exchanged by cesium. ZrP_2O_7 may likely be a selective ion exchanger for removal of ^{137}Cs directly from strong acid HLLW.

Acknowledgments The authors are thankful to colleagues in the project team of the Department of radiochemistry, China Institute of Atomic Energy.

References

- R.C. Ewing, W.J. Weber, F.W. Clinard Jr, Radiation effects in nuclear waste forms for high-level radioactive waste. *Prog. Nucl. Energy* **29**(2), 63–127 (1995). doi:10.1016/0149-1970(94)00016-Y
- K. Ikeda, S. Koyama, M. Kurata, Technology readiness assessment of partitioning and transmutation in Japan and issues toward closed fuel cycle. *Prog. Nucl. Energy* **74**, 242–263 (2014). doi:10.1016/j.pnucene.2013.12.009
- H.S. Junga, S. Choia, I.S. Hwanga, Environmental assessment of advanced partitioning, transmutation, and disposal based on long-term risk-informed regulation: PyroGreen. *Prog. Nucl. Energy* **58**, 27–38 (2012). doi:10.1016/j.pnucene.2012.02.003
- M. Salvatores, G. Palmiotti, Radioactive waste partitioning and transmutation within advanced fuel cycles: achievements and challenges. *Prog. Part. Nucl. Phys.* **66**, 144–166 (2011). doi:10.1016/j.pnpnp.2010.10.003
- E.M. González-Romero, Impact of partitioning and transmutation on the high level waste management. *Nucl. Eng. Des.* **241**, 3436–3444 (2011). doi:10.1016/j.nucengdes.2011.03.030
- T. Tsukada, K. Uozumi, T. Hijikata et al., Early construction and operation of highly contaminated water treatment system in Fukushima Daiichi Nuclear Power Station (I)—ion exchange properties of KURION herschelite in simulating contaminated water. *J. Nucl. Sci. Technol.* **51**, 886–893 (2014). doi:10.1080/00223131.2014.921582
- K. Shakir, M. Sohsah, M. Soliman, Removal of cesium from aqueous solutions and radioactive waste simulants by coprecipitate flotation. *Sep. Purif. Technol.* **54**, 373–381 (2007). doi:10.1016/j.seppur.2006.10.006
- L.H. Delmau, P.V. Bonnesen, B.A. Moyer, A solution to stripping problems caused by organophilic anion impurities in crown-ether-based solvent extraction systems: a case study of cesium removal from radioactive wastes. *Hydrometallurgy* **72**, 9–19 (2004). doi:10.1016/S0304-386X(03)00120-8
- D.R. Raut, P.K. Mohapatra, M.K. Choudhary, Evaluation of two calix-crown-6 ligands for the recovery of radio cesium from nuclear waste solutions: solvent extraction and liquid membrane studies. *J. Membr. Sci.* **429**, 197–205 (2013). doi:10.1016/j.memsci.2012.11.045

10. J.K. Kim, J.S. Kim, Y.G. Shul, Selective extraction of cesium ion with calyx [4] arene crown ether through thin sheet supported liquid membranes. *J. Membr. Sci.* **187**, 3–11 (2001). doi:[10.1016/S0376-7388\(00\)00592-5](https://doi.org/10.1016/S0376-7388(00)00592-5)
11. A.Y. Zhang, J.Y. Li, Y. Dai, Development of a new simultaneous separation of cesium and strontium by extraction chromatograph utilization of a hybridized macroporous silica-based functional material. *Sep. Purif. Technol.* **127**, 39–45 (2014). doi:[10.1016/j.seppur.2014.02.022](https://doi.org/10.1016/j.seppur.2014.02.022)
12. W.H. Duan, J. Chen, J.C. Wang, Application of annular centrifugal contactors in the hot test of the improved total partitioning process for high level liquid waste. *J. Hazard Mater.* **278**, 566–571 (2014). doi:[10.1016/j.jhazmat.2014.06.049](https://doi.org/10.1016/j.jhazmat.2014.06.049)
13. R.R. Sheha, Synthesis and characterization of magnetic hexacyanoferrate (II) polymeric nanocomposite for separation of cesium from radioactive waste solutions. *J. Colloid Interf. Sci.* **388**, 21–30 (2012). doi:[10.1016/j.jcis.2012.08.042](https://doi.org/10.1016/j.jcis.2012.08.042)
14. Z. Chen, Y. Wu, Y.Z. Wei, Cesium Removal from high level liquid waste utilizing a macroporous silica-based calix[4]arene-R14 adsorbent modified with surfactants. *Energy Procedia* **39**, 319–327 (2013). doi:[10.1016/j.egypro.2013.07.219](https://doi.org/10.1016/j.egypro.2013.07.219)
15. M.R. Awual, S. Suzuki, T. Taguchi, Radioactive cesium removal from nuclear wastewater by novel inorganic and conjugate adsorbents. *Chem. Eng. J.* **242**, 127–135 (2014). doi:[10.1016/j.cej.2013.12.072](https://doi.org/10.1016/j.cej.2013.12.072)
16. E.H. Borai, R. Harjula, Leena malinen, Efficient removal of cesium from low-level radioactive liquid waste using natural and impregnated zeolite minerals. *J. Hazard Mater.* **172**, 416–422 (2009). doi:[10.1016/j.jhazmat.2009.07.033](https://doi.org/10.1016/j.jhazmat.2009.07.033)
17. A. Clearfield, J.A. Stynes, The preparation of crystalline zirconium phosphate and some observations on its ion exchange behavior. *J. Inorg. Nucl. Chem.* **26**, 117–129 (1964). doi:[10.1016/0022-1902\(64\)80238-4](https://doi.org/10.1016/0022-1902(64)80238-4)
18. L. Kullberg, A. Clearfield, On the mechanism of ion exchange in zirconium phosphates—35. An equilibrium study of Na + Cs + H⁺ exchange on crystalline α -zirconium phosphate. *J. Inorg. Nucl. Chem.* **43**, 2543–2548 (1981). doi:[10.1016/0022-1902\(81\)80298-9](https://doi.org/10.1016/0022-1902(81)80298-9)
19. K. Lv, L.P. Xiong, Y.M. Luo, Ion exchange properties of cesium ion sieve based on zirconium molybdopyrophosphate. *Colloid Surface A.* **433**, 37–46 (2013). doi:[10.1016/j.colsurfa.2013.04.061](https://doi.org/10.1016/j.colsurfa.2013.04.061)
20. K. Lv, Y.M. Luo, L.P. Xiong, Studies on ion exchange behavior of cesium into zirconium molybdopyrophosphate and its application as precursor of cesium ion sieve. *Colloid Surf. A.* **417**, 243–249 (2013). doi:[10.1016/j.colsurfa.2012.09.037](https://doi.org/10.1016/j.colsurfa.2012.09.037)
21. S.A. Shady, Selectivity of cesium from fission radionuclides using resorcinol–formaldehyde and zirconyl-molybdopyrophosphate as ion-exchangers. *J. Hazard. Mater.* **167**, 947–952 (2009). doi:[10.1016/j.jhazmat.2009.01.084](https://doi.org/10.1016/j.jhazmat.2009.01.084)
22. H.Y. Zhang, R.S. Wang, CSh Lin, A new ecomaterial zirconyl molybdopyrophosphate for the removal of 137Cs and 90Sr from HLLW. *J. Radioanal. Nucl. Chem.* **247**, 541–544 (2001). doi:[10.1023/A:1010630510267](https://doi.org/10.1023/A:1010630510267)
23. H.Y. Zhang, S.L. Wang, R.S. Wang, New ecomaterial zirconyl molybdopyrophosphate for cesium removal from HLLW. *Acta Phys. Chim. Sin.* **16**, 952–955 (2000). doi:[10.3866/PKU.WHXB20001016](https://doi.org/10.3866/PKU.WHXB20001016)
24. X.C. Fu, W.X. Shen et al., *Physical Chemistry*, vol. 2 (Higher Education Press, Beijing, 2006), pp. 361–375